CHAPTER 3

PHOTOPHYSICAL STUDIES ON THE INTERACTION OF ANS, TNS & MC540 WITH ORMOSIL NANOPARTICLES

In this chapter we describe the results of our studies carried out on interaction of ORMOSIL NPs (SiNPs) with negatively charged fluorophores 8-Anilino-1-naphthalenesulfonate (ANS), 6-p-toluidino-2-napthalenesulphonate (TNS) and Merocyanine 540 (MC540). The effect of binding, of these dyes with SiNPs, on their excited state processes is discussed. We also compare the photophysics of MC540 with its complex with SiNP-VA and liposome. The photostability studies of the MC540-NP complex and its light induced toxicity in cancer cells are also presented.

3.1 Introduction

Negatively charged fluorophores like ANS, TNS and MC540, whose excited state processes are dominated by a significant change in structure due to processes such as

Work discussed in this chapter resulted in the following publication:

1. 'Interaction of ANS and TNS with organically modified silica nanoparticles in aqueous media' B. Jain, A. Uppal, P. K. Gupta, K. Das, *Advanced Science Letters*, Vol. 3, pp. 225-230 (2010).

2. 'Light induced toxicity of merocyanine-540-silica nanoparticle complex,' K. Das, A. Uppal, B. Jain, B. Bose, and P. K. Gupta, *Journal of Nanoscience and Nanotechnology*, Vol. 9, pp. 1-4 (2009).

electron transfer or photoisomerism, can get affected on binding with SiNPs due toelectrostatic interaction. The fluorescence of ANS and TNS is known to be markedly sensitive to the environment polarity and viscosity [107, 83, 84,108, 87]. While, these are almost nonfluorescent in a polar medium like water, non-polar/viscous environments cause the fluorescence to be increased by several orders of magnitude. This has been attributed to twisted intramolecular charge transfer (TICT) from the anilino group (for ANS) or p-toluidino group (for TNS) to the sulphonate group. The chemical structures of ANS and TNS are shown in Fig. 3.1. In polar solvents, this nonradiative TICT process is very efficient leading to weak fluorescence. In nonpolar medium the TICT process is suppressed which leads to the enhancement of fluorescence. The intensity, quantum yield and lifetime of ANS fluorescence depends on the geometry of the phenyl ring twist about the bond connecting it to the naphthalene moiety [109]. These dyes have been extensively utilized for the characterization of protein binding sites. D. Matulis et al showed that ANS binds stronger to BSA than inorganic anions [110]. Enhanced binding to protein has been partially ascribed to the large anilinonaphthalene organic moiety of ANS as well as the ion pair formation. Binding to proteins thus comes from both its nonpolar anilinonaphthalene and the negatively charged sulfonate groups (Fig. 3.1).

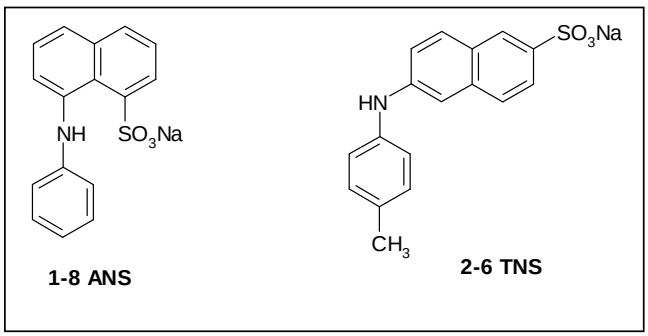

Figure 3.1 *Chemical structures of aniline naphthalene sulphonates used in this study*

MC540 is a lipophilic, cyanine dye which readily binds to membranes, macromolecules and organized assemblies [88, 111, 112, 113] and has been used for

photodynamic inactivation of enveloped viruses in blood products and leukaemia cells [114, 115]. Its optical properties are reported to be very sensitive to environmental polarity, viscosity etc. [87] and therefore it has been used in variety of applications such as trans membrane potential monitoring in biological samples [116], investigating lipid packing in membranes [117, 118], etc.

In aqueous solution MC540 exists as a mixture of monomers and dimers. While the monomeric form of the dye is weakly fluorescent, its dimeric form is nonfluorescent [86, 119]. The relatively low singlet oxygen quantum yield of the dye is ascribed to the efficient excited state photoisomerization around the central double bond (Fig. 3.2).

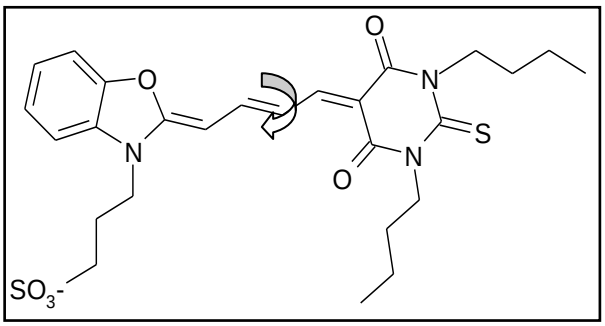

Figure 3.2 *Photoisomerization of MC540 around the central double bond*

This photoisomerization process accounts for the main non-radiative decay pathway for MC540 in the excited state [88]. In addition, the dye is also observed to be readily photodegradable in aqueous solution which might result from the generation of the radical species involved during the photoisomerism process. Therefore, a reduction in the photoisomerization rate by appropriate binding that hinders intramolecular motion may enhance the singlet oxygen yield and photostability of the dye. Indeed it has been observed that the singlet oxygen quantum yield of the drug bound to liposomes is ~ 20 times greater than the free drug [120]. Another simple approach to achieve a reduction in the photoisomerization rate of the drug will be to restrict its intramolecular motion by electrostatically binding the drug with positively charged nanoparticles. In this

chapter we have first used ANS and TNS to photophysically characterize the SiNP-V and SiNP-VA and then studied the photophysics of these probes in the SiNP environments and protein and investigated the role of 3-amino-propyl group in the binding process. We also studied the interaction of MC540 with SiNP-VA suspended in aqueous environment and compared its photophysics with that of only dye and dye complexed with liposome (model membrane). This was followed by photostability studies of dye-NP complex and its light induced toxicity in cancer cells.

3.2 Experimental Methodology

For photophysical studies:

Details of the nanoparticles SiNP-V and SiNP-VA and liposomes used for our studies are given in chapter 2. Bovine serum albumin (BSA), ANS, TNS and MC540 were purchased from Sigma and used as received. The experimental set used for Zeta potential measurements, and steady state absorption and emission measurements are detailed in chapter 2. Emission lifetimes and anisotropies were recorded by excitation at the second harmonic of Ti-sapphire femtosecond laser operating at wavelength 740 nm (to excite ANS and TNS at 370 nm) and 900 nm (to excite MC540 at 450 nm) and using TCSPC (details are in chapter 2 and ref.121). For all experiments performed the concentration of ANS, TNS and MC540 were fixed at 10 μM and 1μM respectively. The concentrations of BSA and SiNP were used as 15 μM and ~1.0 mg/mL respectively.

For Cellular studies:

Phototoxicity studies were done using MCF cells purchased from national centre for cell sciences, Pune, India. Experimental samples were prepared by Dr. Abha Uppal, details are given in reference 122. For irradiation, cells in monolayer were kept in phosphate buffer saline (PBS) containing 5 mM glucose. A 450 to 650 nm bandpass filter was used

to select the wavelength of irradiation from the broadband output of a xenon lamp source. Samples were kept at a distance of 30 cm from the light source and the power incident at the sample was measured by an OPHIR power meter (3A sensor head). Following irradiation at different light dose, the media were replaced with fresh growth medium at pH 7.4. After 24 h, MTT assay was performed to determine the cell survival following the method described by Mosman [102] (details are described in chapter 2). Each irradiation experiment was repeated thrice and for each of these experiments a corresponding control experiment in which cells, devoid of drug and SiNP-VA, exposed to similar light dose was also carried out.

3.3 Results and Discussion

The effect of pH on the zeta potential of the SiNP's is shown in Fig. 3.3.

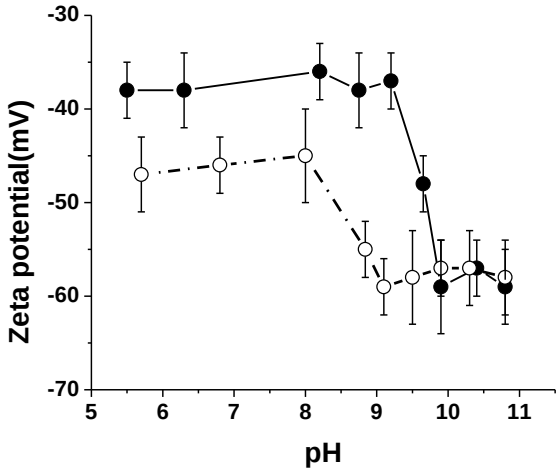

Figure 3.3 *pH titration curves: Variation of zeta potential of SiNP-VA (solid) and SiNP-V (hollow) with pH.*

As shown in the figure, the zeta potential of SiNPs decreases as the pH is changed from ~5.5 to ~11.0. For SiNP-V the zeta potential starts to decrease after pH 8.0 and stabilizes to a value of ~ -58.0 mV above pH 9.0. This change can be attributed to the acid-base equilibrium of the silanol groups present at the surface. It has been earlier reported that

for macroscopic silicon dioxide-water interface the surface silanol groups have two pK_a values one at 4.5 and the other at 8.5 [123]. For SiNP-VA the zeta potential however starts to decrease after pH 9.2 and reaches a minimum of ~ -58.0 mV at pH ~10.0 and stabilizes after that. The observed difference in the trend of zeta potential vs. pH curves may be attributed to the presence of combined acid-base equilibrium of the surface silanol and 3-amino propyl groups present in SiNP-VA. At neutral pH, the zeta potential for SiNP-V is observed to be around -45.0 ± 3.0 mV while that for SiNP-VA is observed to be around -36.0 ± 3.0 mV (Fig. 3.3). This difference in the zeta potential may be attributed to the presence of the 3-amino propyl groups at the surface in SiNP-VA. At pH 7.0 the amine groups, present at the surface, are expected to be positively charged as the pK_a value of the 3-aminopropyl group of APTS is ~9 [124]. This positive charge neutralizes to some extent the negative charges caused by the presence of surface silanol ($Si\text{-}O^-$) groups and increases the zeta potential for SiNP-VA (making it more positive) compared to SiNP-V.

3.3.1 Spectroscopic studies of ANS and TNS with SiNP-V and SiNP-VA

The fluorescence properties of ANS and TNS in the presence of ~1.0 mg/mL SiNP-V and SiNP-VA in aqueous medium at neutral pH are shown in Fig. 3.4 and the corresponding fluorescence parameters are provided in Table 3.1. For comparison, the fluorescence of these probes in neutral water and in the presence of 15μM BSA are also provided in Fig. 3.4. The emission intensity and lifetime of the probes follow the order: water < SiNP-V < SiNP-VA < BSA. As noted earlier, the fluorescence of both ANS and TNS are dependent on the polarity of the surrounding environment [107, 83, 84,108]. In the highly polar medium, water, the fluorescence properties of both probes are weak due to efficient nonradiative TICT process. Compared to water, a marginal enhancement in fluorescence was observed in the presence of SiNP-V and a significant enhancement was observed in the presence of SiNP-VA indicative of an interaction between the probes and SiNP-VA.

Although the interior of both nanoparticles are reported to be hydrophobic [51, 124], the fluorescence properties of the probes in the presence of these nanoparticles suggest that surface property of the nanoparticle plays an important role in the probe-nanoparticle interaction.

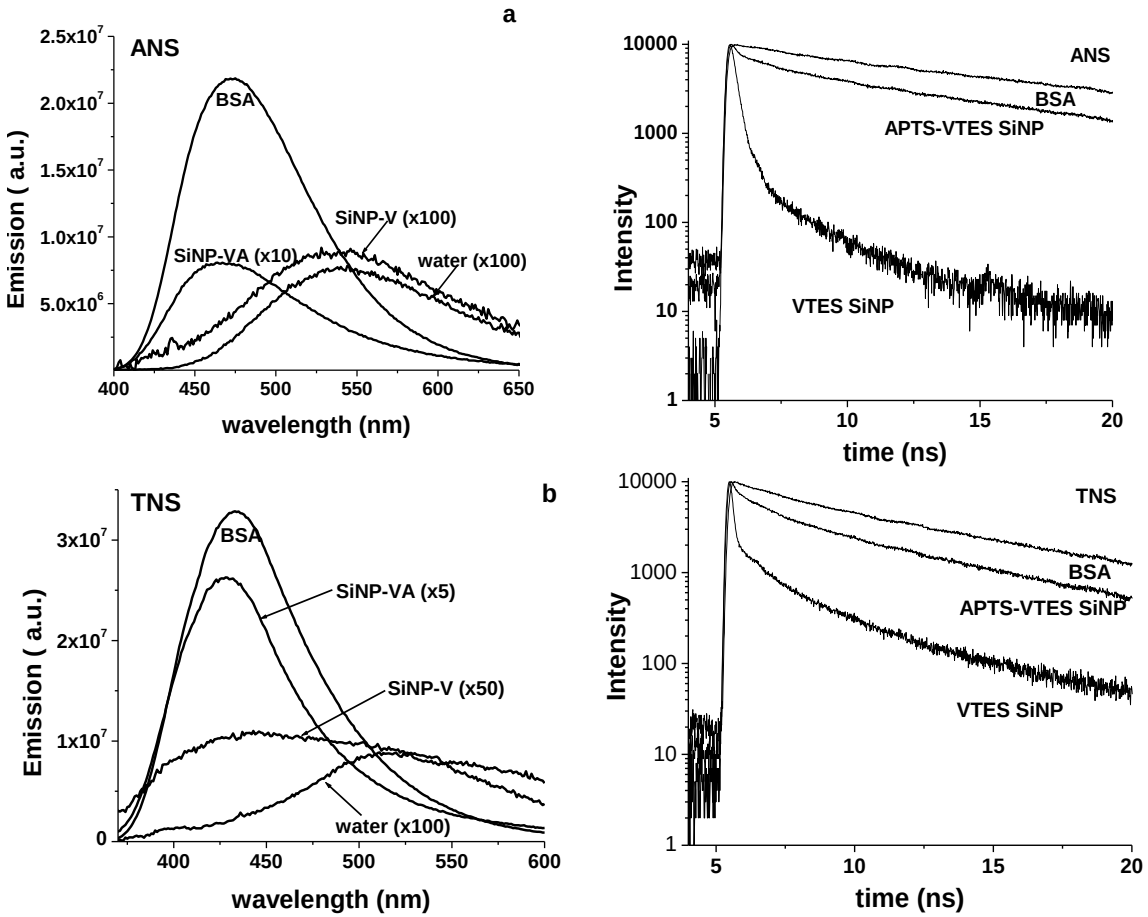

Figure 3.4 *Fluorescence (λ_{ex} = 370 nm) emission (left) and lifetimes (right) of ANS (a) and TNS (b) in presence of BSA, SiNP-V, SiNP-VA and water. Some spectra are magnified for comparison.*

Significant interaction between the negatively charged probes and SiNP-VA having a positive zeta potential value as compared to SiNP-V is indicative of an electrostatic interaction mechanism operative in the case of SiNP-VA. This may be attributed to electrostatic binding between the negatively charged ANS & TNS with positively charged 3-amino propyl groups present in SiNP-VA. Since the pK_a of the 3-amino propyl group is reported to be ~9.0, the presence of electrostatic interaction mechanism can be tested by

Table 3.1 *Fluorescence parameters of ANS and TNS in different environments*

System	Em. Max. (nm)	QY	Lifetime (ns)								k_{nr} ($x10^{-9}s$)	k_r ($x10^{-9}s$)
			χ^2	τ_1	a_1	τ_2	a_2	τ_3	a_3	τ_{av}		
10 µM ANS in												
Water	540	0.004[a]	0.20[a]								5.0	0.015
BSA	472	0.580	1.25	--	--	9.00	0.28	15.0	0.72	13.3	0.03	0.044
SiNP-VA	465	0.020	1.15	--	--	2.30	0.13	11.00	0.87	9.9	0.10	0.002
SiNP-V	535	0.004	1.00	0.20	0.79	1.25	0.10	4.30	0.11	0.8	1.25	0.005
Isopropanol	470	0.480	1.00	--	--	--	--	7.40	100	7.4	0.07	0.065
Isopropanol + 2.36 (M) VTES	472	0.400	1.10	--	--	--	--	6.40	100	6.4	0.09	0.063
Isopropanol + 2.14 (M) APTS	476	0.234	1.10	--	--	1.40	0.21	4.30	0.79	3.7	0.21	0.063
10 µM TNS in												
Water	515	0.001[a]	0.06[a]								16.65	0.02
BSA	433	0.256	1.13	--	--	2.00	0.11	8.20	0.89	7.5	0.10	0.034
SiNP-VA	427	0.020	1.10	--	--	1.50	0.23	6.90	0.78	5.7	0.17	0.004
SiNP-V	445	0.003	1.10	0.20	0.36	1.40	0.28	5.60	0.36	2.5	0.40	0.001
Isopropanol	418	0.414	1.10	--	--	--	--	5.60	100	5.6	0.10	0.074
Isopropanol + 2.36 (M) VTES	425	0.410	1.10	--	--	--	--	4.80	100	4.8	0.12	0.085
Isopropanol + 2.14 (M) APTS	427	0.087	1.10	--	--	1.30	0.79	2.40	0.21	1.5	0.61	0.058

[a] *Data taken from reference 84* and 125.

varying the pH of the medium. Consistent with the fact that neutralization of amino groups should result in a decrease in the electrostatic binding and hence fluorescence, the integrated emission intensity of the probes was observed to decrease after pH ~9.0 as shown in Fig. 3.5, a &b.

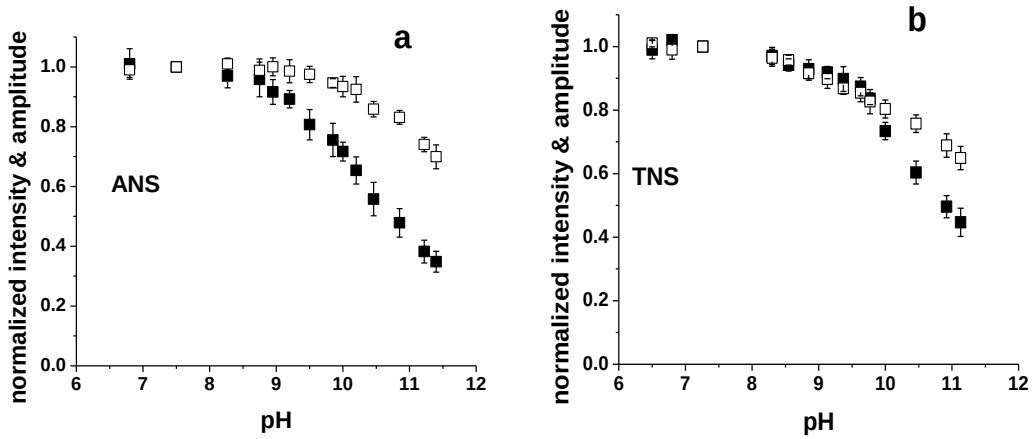

Figure 3.5 *pH titration curves: Variation of fluorescence (λ_{ex} = 370 nm) with pH of ANS (a) and TNS (b) in presence of SiNP-V (solid) and SiNP-VA (hollow). The black squares represent the normalized changes in integrated emission intensity and the hollow squares represent the normalized changes in the amplitudes of the long lifetime component obtained from a global fit. Please see text for more details.*

The fraction of probe molecules bound to SiNP-VA can also be estimated from the amplitude of the long lifetime component. However, since the decays were found to be wavelength dependent, the amplitude of the long lifetime component were obtained by collecting the decay traces over the 'whole band' at different pH, and then by performing a global fit of the decay traces. The changes in the number of bound probes with pH estimated in this way were also observed to be consistent with changes observed for integrated emission intensity (hollow squares in Fig. 3.5).

It is thus clear that electrostatic interaction plays an important role in the binding process. When we compared fluorescence properties of the probes bound to BSA and SiNP-VA some interesting observations were revealed (Fig. 3.4 & Table 3.1). The

emission maxima of the probes were observed to be distinctly blue shifted when they were bound to SiNP-VA indicating that in this case the probes were experiencing a less polar environment than BSA. This implies that the other emission properties like emission intensity and lifetime should be at least equal if not greater than that observed in the presence of BSA. Fluorescence decay of the probes bound to either BSA or SiNP-VA could be satisfactorily fitted with a double exponential. Compared to BSA when the probes are bound to SiNP-VA the average lifetimes of the probes were observed to be marginally smaller (~1.3 times each) while the quantum yield of emission was observed to be significantly smaller (~29 and ~13 times for ANS and TNS respectively). These results show that compared to protein the binding with SiNP-VA affects the nonradiative rates marginally but decreases the radiative rates significantly (20 and 11 times for ANS and TNS respectively). This is indicative of a quenching mechanism present in SiNP-VA.

For understanding this aspect better, fluorescence of ANS & TNS in isopropanol and with VTES and APTS was studied. As shown in Fig. 3.6, the strong fluorescence of ANS & TNS in isopropanol is quenched by both VTES and APTS and the nature of quenching is both static and dynamic (corresponding data presented in Table 3.1). The quenching by APTS is more severe than VTES. This may be attributed to the amine groups present in APTS, which are well known quenchers of fluorescence. This result suggests that fluorescence of these probes, when bound to SiNP, may get quenched.

Although a comparison of the radiative and nonradiative decay rates of the probes bound to SiNP-VA indicated that quenching is primarily static in nature, we further investigated this aspect by studying the fluorescence anisotropy decay of the probes when bound to SiNP-VA and compared that with BSA. The anisotropy decays are provided in Fig. 3.7 and the corresponding parameters are provided in Table 3.2. The data can be fitted satisfactorily to a bi-exponential decay model represented by:

$$r(t) = r_o [a_1 \exp(-t/\tau_1) + a_2 \exp(-t/\tau_2)]$$

where r_o is the initial anisotropy and τ_1 and τ_2 are the time constants for the decay of r_o is

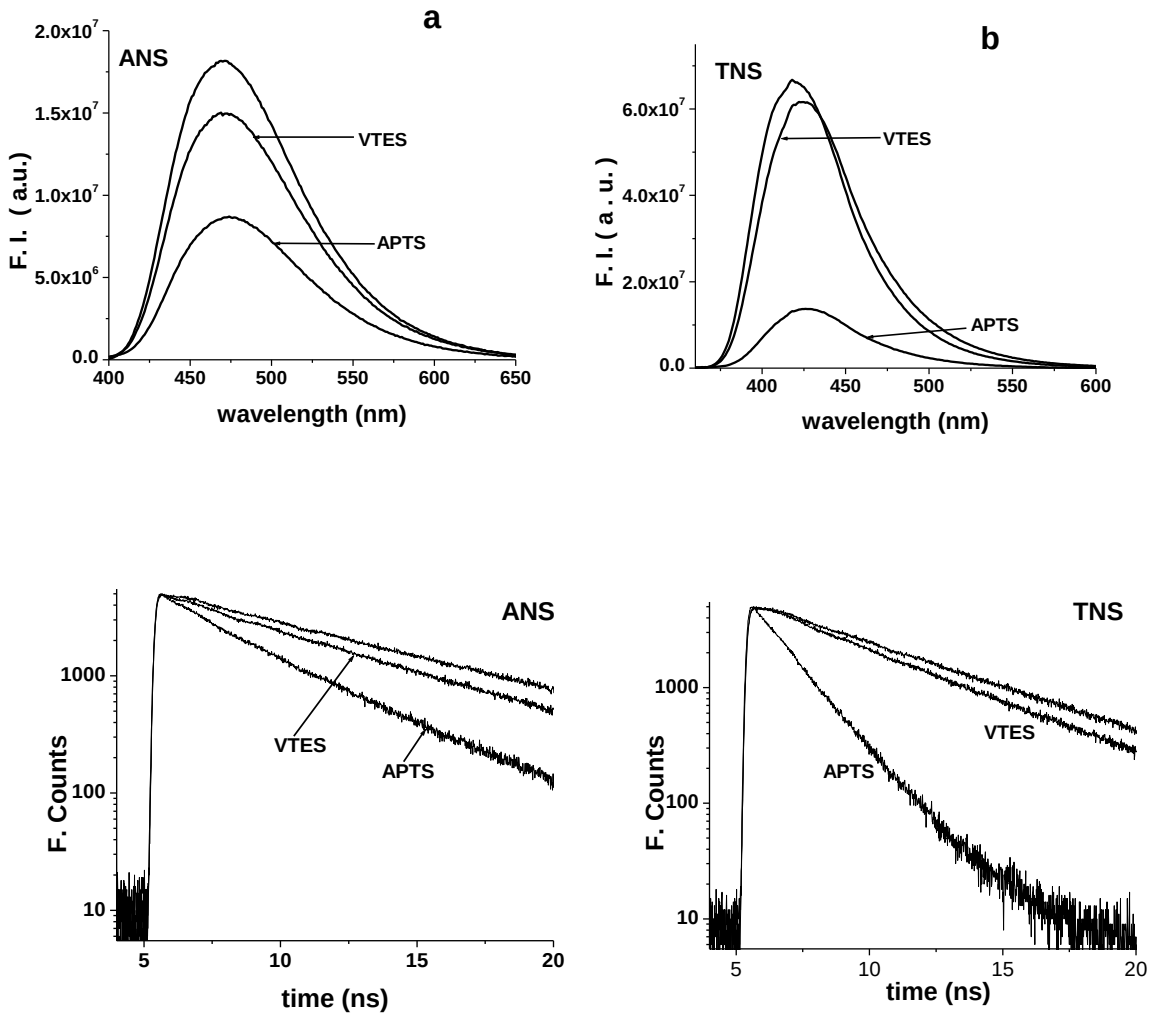

Figure 3.6 *Fluorescence (λ_{ex} = 370 nm) emission (top) and lifetimes (bottom) of ANS (a) and TNS (b) in isopropanol, and isopropanol containing 2.36 (M) VTES and 2.14 (M) APTS.*

the initial anisotropy and τ_1 and τ_2 are the time constants for the decay of r_o having pre-exponential factors of a_1 and a_2 respectively. The component τ_1 represents the overall factors responsible for faster dephasing of anisotropy including local motion and quencing of the fluorescence of the probe. The slower component τ_2 represents the overall motion of the probe-BSA or probe-SiNP complex.

For protein bound probe, the overall motion is characterized by a time constant of 40-50 ns as observed earlier [109]. For probe bound to SiNP-VA (whose size is much larger than BSA) we note that the experimental time window is not sufficient enough to

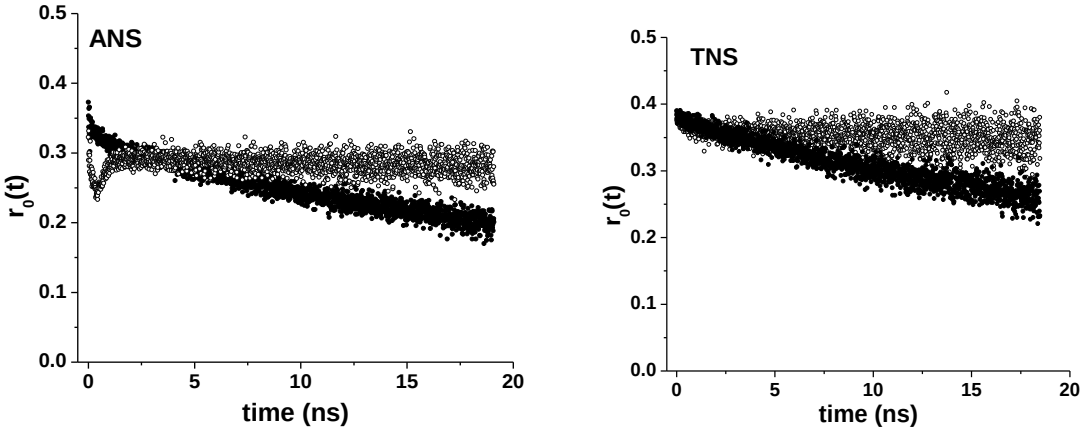

Figure 3.7 *Fluorescence (λ_{ex} = 370 nm) anisotropy decay curves along with fitted curves of ANS (left) and TNS (right) in presence of BSA and SiNP-VA. The fitted anisotropy parameters are given in Table 3.2.*

give a correct estimate of the overall motion of the nanoparticle. The initial fluorescence anisotropy decay of ANS bound to either BSA or SiNP-VA shows distinctly a fast component. For SiNP-VA, r(t) initially shows a dip and then rise. This type of anisotropy decay has been previously observed for fluorophores having very fast and slow rotational motions of the excited dipole [126 ,127].

Table 3.2 *Anisotropy parameters of ANS and TNS in different environments*

System	a_1[a]	τ_1 (ns)	τ_2 (ns)	r_0
10 µM ANS in				
SiNP-VA	0.30	0.20	∞[b]	0.39
BSA	0.15	1.5	40.0	0.33
10 µM TNS in				
SiNP-VA	0.07	1.0	∞[b]	0.38
BSA	0.30	5.0	50.0	0.38

[a] *Pre-exponential factor*

[b] *The time window is not sufficiently long enough to measure this time constant and hence it is shown as infinity.*

For SiNP-VA bound ANS the faster component comes out to be ~200 ps accounting for 30% of anisotropy decay whereas for BSA bound ANS this is 1.5 ns accounting for 15% of anisotropy decay. We note here that due to the limited time resolution (~200 ps) of our

setup the estimation of the faster component of ANS bound to SiNP-VA is only approximate, nevertheless its presence shows significant dynamic fluorescence quenching of ANS when compared to that in BSA.

In contrast the anisotropy decay of TNS in these two systems clearly does not show the presence of a fast component (Table 3.2). A biexponential fitting of the anisotropy decay of TNS bound to SiNP-VA shows no significant fast component whereas when it is bound to BSA it shows the presence of a 5 ns component with a 30% weight, which is indicative of the local motion of the protein bound probe. Thus, for TNS bound to the nanoparticle anisotropy experiments suggests that only static quenching mechanism is operative.

The significantly higher decrease in quantum yield and hence the radiative rate as well as observation of a faster anisotropy dephasing time in ANS compared to TNS in SiNP-VA suggests that in addition to quenching induced by APTS and/or VTES the structure of the probes might also be responsible. The non-radiative TICT process, which involves twisting between the donor and the rest of the molecule, is expected to be affected differently for ANS and TNS when they are bound to the 3-amino propyl groups present at the surface of SiNP-VA. For ANS, the donor and acceptor are on the same side of the naphthalene moiety but for TNS they are on the opposite side (Fig. 3.1). The presence and absence of a faster anisotropy dephasing time for ANS and TNS respectively suggests that in addition to the quenching by APTS and/or VTES, the TICT process might be operative in a greater extent in ANS compared to TNS.

3.3.2 Spectroscopic studies of MC540 with SiNP-VA

The absorption, emission and fluorescence lifetimes of MC540 in aqueous medium in the presence and absence of SiNP are shown in Fig. 3.8. In aqueous medium the absorption band of the dye is broad with two peaks centered at 505 and 536 nm. The emission peak of the free dye is at 570 nm having a quantum yield of 0.03 and lifetime of ~100 ps.

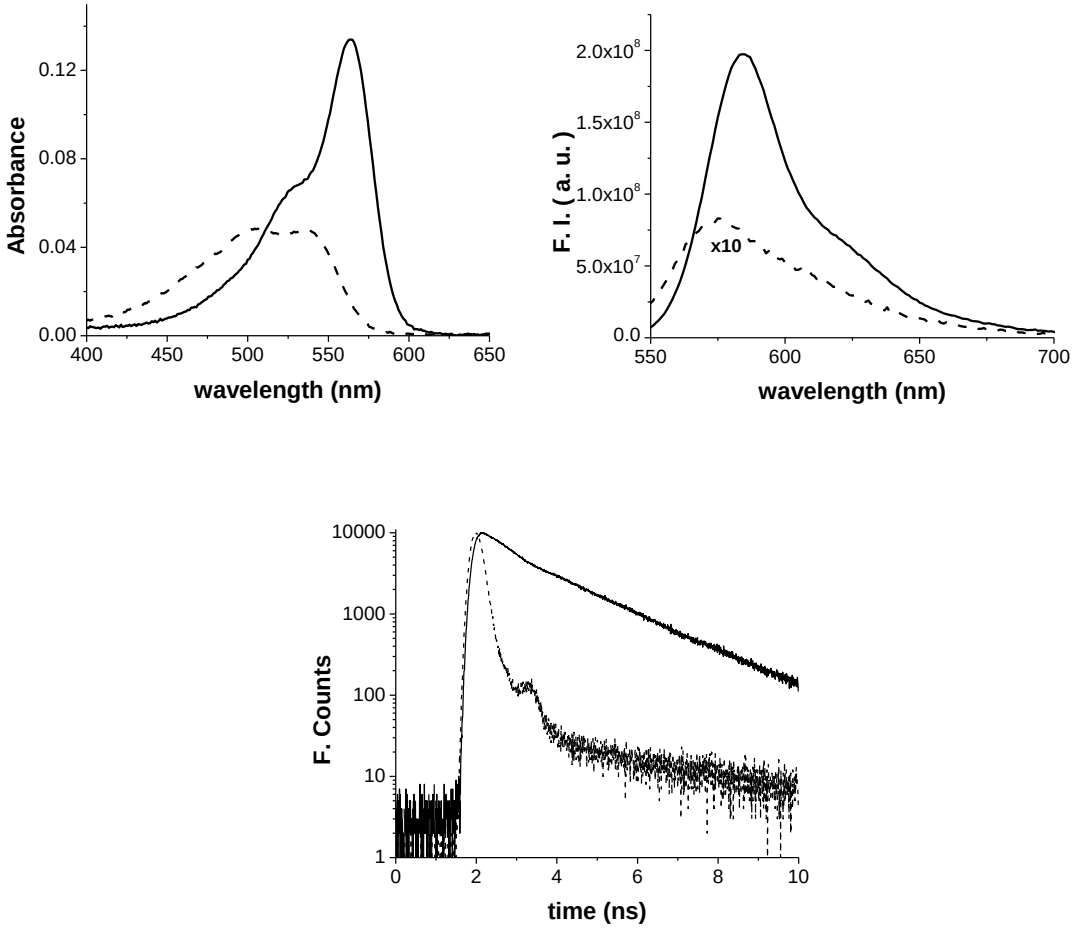

Figure 3.8 *Absorption (top left), emission (top right, λ_{ex} = 530 nm) and fluorescence decay curves (bottom, λ_{ex} = 450 nm) of MC540 in aqueous medium (dotted curve) and in presence of ~940 µgm/mL SiNP (solid curve)*

In the presence of SiNP the absorption of the dye gets considerably modified with a peak at 563 nm and a shoulder on the blue side (Fig. 3.8). Further, the emission is red shifted to 583 nm, with intensity increasing by ~18 times and the lifetime increasing to 1.5 ns (15 times increase).

These results suggest that there is a strong interaction between the dye and SiNP. This interaction is probably due to electrostatic binding between the oppositely charged species. To get more insight about this binding we have performed a fluorescence titration (intensity & lifetime) of the dye with increasing SiNP concentration, the results of which are described in Fig. 3.9.

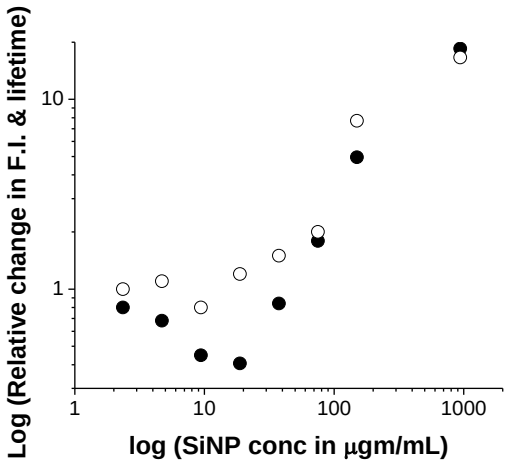

Figure 3.9 *Relative integrated emission intensity (solid) and average lifetimes (hollow) of MC540 in presence of varying amounts of SiNP added. The values plotted are normalized to that of the dye in water. The X and Y axes are plotted in a logarithmic scale for clarity*.

As shown in the Fig.3.9, the fluorescence intensity of MC540 decreases with increasing concentration of SiNP till a concentration of ~19 μg/mL and increases beyond this concentration. In contrast, the lifetimes with increasing SiNP concentration remains roughly constant (~0.1 ns, which falls within the instrument response function of the lifetime system) till a SiNP concentration of ~19 μg/mL and increases progressively thereafter. The absorption and emission parameters of the dye in aqueous medium, in the presence of SiNP and in the presence of liposomes (for comparison) are presented in Table 3.3.

Table 3.3 *Absorption & fluorescence parameters for MC540 in different environments*

System	Absorption (nm)	Emission				
		Peak (nm)	Quantum yield	Average lifetime (ns)	k_r ($x10^{-9}s^1$)	k_{nr} ($x10^{-9}s^{-1}$)
MC540/H_20	505/536	570	0.03	0.10	0.30	9.70
Liposome	565	583	0.49	1.6	0.31	0.32
SiNP	563	583	0.53	1.5	0.31	0.28

It can be seen that the fluorescence enhancement of the dye are due to the reduction in the nonradiative rates and are comparable in the presence of SiNP and liposomes. These results suggest a reduction in the photoisomerization rate of MC540 in presence of SiNP that is likely to result due to the restriction on the intramolecular motion of the dye bound at the SiNP surface.

3.3.3 Light induced photostability and phototoxicity of MC540 and its SiNP complex

The photostability of the free dye and dye-SiNP complex in aqueous medium was studied under visible light irradiation for three different light doses by monitoring the change in the absorption spectra and is described in Fig. 3.10.

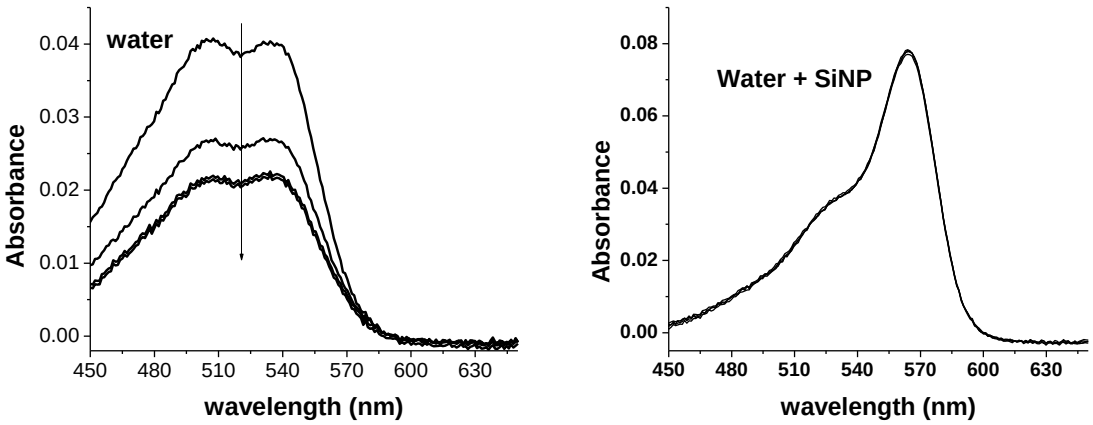

Figure 3.10 *Photobleaching of MC540 in aqueous medium in the absence (left) and in the presence of ~940 µgm/mL SiNP (bottom). The irradiation conditions are described in the materials & methods section. The arrow in the top panel represents increasing light dose of 0, 1.8, 3.6 and 5.4 kJ/m*^{2}

At a light dose of 1.8 kJ/m^2 there is a significant decrease in the absorbance of the free dye (~ 37 %) in aqueous medium and it seems to saturate to ~ 45 % of initial value as the dose is increased to 5.4 kJ/m^2. This implies that almost half of the dye population has been photodegraded at a light dose of 5.4 kJ/m^2. In the presence of SiNP there is no change in the absorption spectra of the dye at these light doses which implies that the

photostability of the dye is significantly improved upon binding with SiNP. This is expected from the results presented in Fig. 3.8 which suggest that the binding lowers the photoisomerization rate of the dye bound to the SiNP surface.

Studies on cellular toxicity were carried out using MCF cells. No statistically significant dark toxicity was observed for the dye (upto 10 μM), SiNP (upto 50 μgm/mL) and MC540-SiNP complex having a dye concentration of 1-10 μM and SiNP concentration of 10-50 μgm/mL. These cells were irradiated, with a MC540 concentration of 1 μM, SiNP concentration of 20 μgm/mL, and MC540-SiNP mixture where dye concentration was kept at 1 μM and SiNP at 20 μgm/mL. The results of the percentage cell survivals (with respect to control) under irradiation at different light dose for the free dye, SiNP and dye-SiNP complex are given in Table 3.4.

Table 3.4 *Light induced toxicity of MC540, SiNP and MC540-SiNP complex against MCF-7 cells*[a]

System	Concentration of MC540 & SiNP	Light dose 1.8 kJ/m^2	Light dose 3.6 kJ/m^2	Light dose 5.4 kJ/m^2
Only MCF-7 cells	-	100 %	100 %	100 %
Cells + MC540	1 μM	96±2	93±3	89±2
Cells + SiNP	20 μgm/mL	92±3	85±3	79±4
Cells + MC540-SiNP	1 μM MC540 & 20 μgm/mL SiNP	71±3	62±4	56±2

[a]*The values shown are the mean and standard deviation of three experiments performed. For each set of experiment the control was taken as MCF-7 cells against which the percentage cell survival was obtained.*

For free dye, at 1 μM concentration very modest light dose dependent cell killing is observed. For SiNP a slightly higher toxicity is observed. This difference in cell survival for free dye and SiNP is significant to a *p* value of < 0.017 for a light dose of 5.4 kJ/m^2. It is unclear at this point why SiNP by itself leads to light induced toxicity. Results of previous studies on the dark toxicity of SiNP are also a bit ambiguous [128, 129]. Luminescent SiNPs (doped with fluorescent dyes, size 50 nm) did not lead to significant toxicity below a concentration of 0.1 mg/mL on human lung epithelial cells [128]. In

another study, it was observed that exposure to SiNP (15 and 46 nm sizes) resulted in a concentration dependent cytotoxicity in cultured human bronchoalveolar carcinoma-derived cells and it was observed to be closely correlated to increased oxidative stress [129].

It is thus essential to study the light induced toxicity of SiNP in greater detail. For the dye-nanoparticle complex the light dose dependent cell killing was observed to be significantly higher compared to that for free dye and SiNP. This is consistent with the expected increase in singlet oxygen yield due to a reduction in the photoisomerization rate.

3.4 Conclusion

The interaction of ANS and TNS with SiNP-V and SiNP-VA in aqueous media was studied by fluorescence spectroscopy. Our results suggest that the binding of these probes with the nanoparticle is due to electrostatic interaction between the negatively charged probes and positively charged 3-amino propyl group. A comparison of the fluorescence properties of these probes bound to nanoparticle and BSA reveals a significant quenching mechanism operative in the nanoparticle environment. The nature of quenching is observed to be probe dependent. Time resolved fluorescence experiments suggests that for TNS quenching is primarily static in nature whereas for ANS the presence of dynamic quenching is suggested. Photophysical studies on interaction of MC540 with SiNP-VA suggest that MC540 binds to SiNP-VA which results in a reduction in the photoisomerization rate of the dye. The light induced toxicity of the dye-nanoparticle complex (tested with MCF cells) is observed to be higher compared to the free dye which is consistent with earlier observations that a reduction in the photoisomerization rate increases the singlet oxygen quantum yield of the dye.